Available online at www.sciencedirect.com

SciVerse ScienceDirect

Ceramics International 39 (2013) 8377–8384

CERAMICS INTERNATIONAL

www.elsevier.com/locate/ceramint

Colloidal stability of dextran and dextran/poly ethylene glycol coated TiO_2 nanoparticles by hydrothermal assisted sol–gel method

Sanaz Naghibi[a,*], Hamid Reza Madaah Hosseini[b], Mohammad Ali Faghihi Sani[b]

[a]Department of Materials Engineering, Science and Research Branch, Islamic Azad University, Tehran, P.O. Box: 14778-93855, Iran
[b]Department of Materials Science and Engineering, Sharif University of Technology, Tehran, P.O. Box: 11365-11155, Iran

Received 6 March 2013; received in revised form 5 April 2013; accepted 6 April 2013
Available online 15 April 2013

Abstract

Colloidal stability of dextran (Dex) and Dex/poly ethylene glycol (PEG) coated TiO_2 nanoparticles (NPs) were investigated. The particles were successfully synthesized by a hydrothermal assisted sol–gel technique. The results of Ultraviolet–visible (UV–vis) spectrophotometry showed that Dex and PEG additions during hydrothermal process (HTP) led to the formation of long-term (more than 60 days) stable colloids, while the addition of dispersants after HTP did not have a significant impact on the colloidal stability of NPs. X-ray diffraction (XRD) and selected area electron diffraction (SAED) analyses proved that PEG and/or Dex coated NPs had less crystallinity than the plain TiO_2. Fourier transform infrared (FTIR) spectroscopy demonstrated the formation of primary bonds between NPs and polymeric dispersants. High-resolution transmission electron microscopy (HRTEM) displayed stable particles with a core-shell structure resulting from coating of NPs by polymeric materials. Thermo gravimetric analysis (TGA) was also utilized to calculate the proportion of NPs to polymeric dispersant.

Keywords: TiO_2 nanoparticle; PEG; Dextran; Hydrothermal assisted sol–gel; Colloidal stability

1. Introduction

Excellent biocompatibility [1,2], high chemical stability [3] and unique photocatalytic properties [4] provided by TiO_2 NPs make them a remarkable candidate for a vast number of applications in the efficient delivery of therapeutic and diagnostic agents [5,6], sonodynamic therapy [7] and photodynamic therapy [8–11]. Various techniques have been used to prepare TiO_2 based components such as mesoporous [12], whisker [11], thin layer [8,13] and nanocomposite powder [14] for different applications. The usage of TiO_2 in the therapeutic and diagnostic fields may be confined due to its poor dispersibility in water and biological serums and subsequent agglomeration and sedimentation of NPs through the tissues. As a result, biodistribution of NPs may be suffered and healthy cell viability may be decreased. To improve the disposition behavior of TiO_2 NPs in biological systems, it is necessary to study surface properties and colloidal stability of TiO_2 NPs [5,15,16]. Some recent studies have focused on surface covering of NPs with polymeric materials in order to prevent the aggregation and sedimentation [7,17–20], reduce their toxicity [7] and improve their biocompatibility [21].

Yamaguchi et al. constructed water-dispersed TiO_2 NPs by chemical adsorption of PEG on the TiO_2 surface [7]. Luo et al. modified TiO_2 NPs by a mixed template of PEG and cetytrimethylammonium bromide (CTAB) at 60 °C using an autoclave. They reported that PEG played a dispersant role in controlling the structure of TiO_2 NPs [18]. Petryshyn et al. studied the effects of benzethonium chloride, sodium dodecylbenzenesulfonate, and 4-(1,1,3,3-(tetram ethylbutyl) phenyl PEG on the zeta potential and stability of aqueous rutile in the pH range of 2–12. They showed that the non-ionic surfactant did not significantly affect the zeta potential and stability of the suspensions. The influence of ionic surfactants on the stability of the suspensions considerably depended on the pH of a medium [19]. Veronovski et al. succeeded in obtaining stable dispersions without formation of large agglomerates of TiO_2 P25 NPs by cationic Gemini surfactant [20].

Other organic materials such as Dex have also been used to increase the dispersion of Fe_3O_4 NPs [14,21]. Dex has been used

*Corresponding author. Tel.: +982147911; fax: +982144868474.
E-mail addresses: naghibi@iaush.ac.ir (S. Naghibi), madaah@sharif.ir (H.R. Madaah Hosseini), faghihi@sharif.ir (M.A. Faghihi Sani).

0272-8842/$ - see front matter © 2013 Elsevier Ltd and Techna Group S.r.l. All rights reserved.
http://dx.doi.org/10.1016/j.ceramint.2013.04.018

as the reducing agent of graphite to synthesize TiO_2–Dex–reduced graphene oxide (RGO) nanocomposite with remarkable photocatalytic activity and photovoltaic response [21].

The aim of this research is to modify the surface condition of as-synthesized TiO_2 NPs via sol–gel, by PEG and/or Dex during HTP, and the formation of chemical bonding among NPs and dispersant agents (PEG and Dex).

2. Experimental procedure

2.1. Starting materials

Titanium tetra isopropoxide (TTIP, > 98%, Merck®, Frankfurt, Germany), isopropyl alcohol (iPrOH, > 99.5%, Merck), hydrochloric acid (HCl, 37%, Merck), triethylamine (TEA, > 99%, Merck), PEG (6000, Merck), Dex (7000, from Leuconostoc mesenteroides, Sigma-Aldrich®, Saint Louis, USA) and distilled water were used as starting materials.

2.2. Preparation and modification of NPs

TiO_2 NPs were prepared by using TTIP as a Ti source, iPrOH as a solvent, HCl as a reagent to adjust pH and distilled water as a hydrolytic agent. The molar ratios of iPrOH to TTIP and water to iPrOH were 2 and 50, respectively. The suspension was continuously stirred at room temperature. Since hydrolysis of Ti^{4+} containing sol does not occur in pH more than 1.75 [22], HCl was added to the suspension to decrease pH to 1.5. In order to increase the pH value to 9 [22], adequate amount of TEA was dropped into the suspension, while stirring.

Two different methods were used to add dispersant to the suspension as described in Fig. 1. In the first method, PEG and/or Dex were added to the suspension and stirred for 5 min. The obtained suspension was then placed in a Teflon recipient inside a stainless steel autoclave. HTP was performed at 100 °C under 6 bars for 18 h. The concentration of TiO_2 in the suspension was calculated about 40 g/L. In order to investigate the stability of NPs in a water base medium, the suspension was diluted and ultrasonically dispersed for 1 h to decrease TiO_2 concentration to 1 g/L. Samples 1, 2 and 3 were designed and prepared by the first method (see Table 1).

In the second method, the suspension, without any dispersant, was placed in the autoclave and underwent HTP, similarly. The suspension containing TiO_2 NPs was ultrasonically dispersed for 1 h and diluted to 1 g/L of TiO_2. Then dispersants were added (according to Table 1) and sonication was continued for 1 h. Samples 4, 5 and 6 were designed and prepared by the second method (see Table 1). As a reference sample, plain TiO_2 suspension was prepared without adding any dispersant. A schematic flowchart of the synthesis methods is summarized in Fig. 2.

2.3. Characterization

The colloidal stability of TiO_2 NPs in water base suspension was evaluated through measuring the absorption by a UV–vis. spectrophotometer (T70, PG Instruments Ltd., Leicestershire, England) in wavelength range of 200–800 nm. To compare the absorption of different samples, the area under the Abs vs. λ curves was measured and determined as the index of colloidal stability. In order to separate the remainder of starting materials and chemical by-products such as triethylamine hydrochloride from the suspension containing PEG and/or Dex coated NPs, dialyze membrane (molecular weight cut-off; MWCO = 5000) against distilled water was utilized.

XRD patterns were obtained by an X-ray diffractometer (D8 advance, Bruker®, Karlsruhe, Germany) using monochromatized Cu-K_α ($\lambda = 1.5418$ Å) radiation.

The functionalization of NPs by PEG and/or Dex was examined by FTIR spectroscopy (65, PerkinElmer®, Massachusetts, USA) in KBr matrix in the range of 4000–400 cm^{-1} using the transmission mode.

Table 1
Preparation methods and dispersant composition of the samples.

Method	First method			Second method		
Samples	1	2	3	4	5	6
PEG to TiO_2 weight ratio	1	0	0.5	1	0	0.5
Dex to TiO_2 weight ratio	0	1	0.5	0	1	0.5

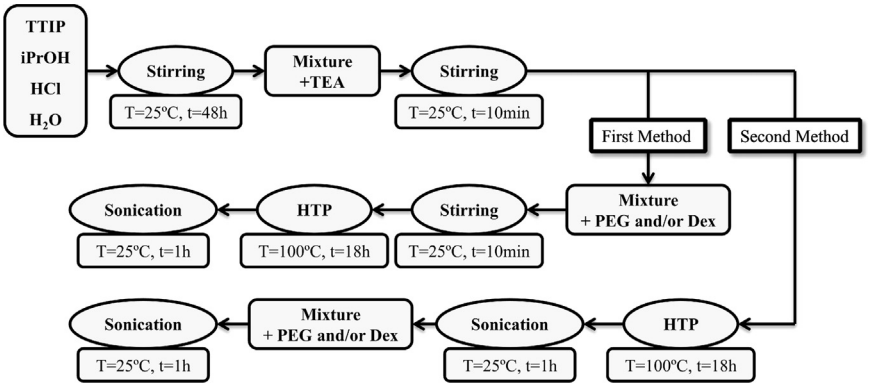

Fig. 1. Synthesis procedures of modified TiO_2 NPs.

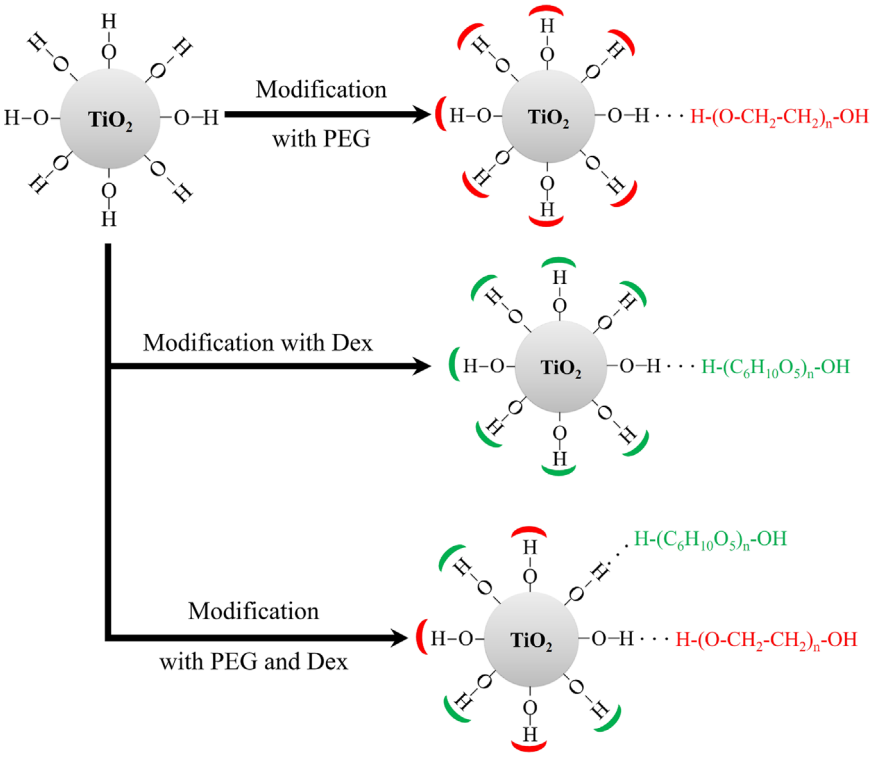

Fig. 2. Schematic illustration for functionalization of TiO_2 NPs with dispersants. Red arcs relate to PEG; H–(O–CH_2–CH_2)$_n$–OH and green arcs refer to Dex; H–($C_6H_{10}O_5$)$_n$–OH.

TEM (Philips®, Amsterdam, Netherlands) with an accelerating voltage of 100 kV and HRTEM (Philips) at 250 kV was utilized for microscopic evaluations. Samples were prepared by dipping a Cu grid into dispersion of the modified NPs in ethanol.

The amount of weight loss of polymeric materials, resulting from heating of conjugated NPs, was also investigated by a thermo gravimeter (503, BAHR®, Hullhorst, Germany). A small amount of specimens weighing about 50 ± 5 mg was held in an alumina crucible and heated under atmospheric conditions (flow rate: 50 mL/min) at a heating rate of 10 °C/min up to 700 °C.

3. Results and discussion

3.1. Effects of dispersing agents and preparing methods on the colloidal stability

Different dispersing agents and preparing methods were appraised to modify TiO_2 NPs. Fig. 3 depicts absorption of the suspensions as a function of relaxation time (0, 24 h, 20 and 60 days), accompanied by their visual dispersion state after 60 days. It is clear that absorbance value immediately after sonication (black columns) was higher in samples 4, 5 and 6 in comparison with that of samples 1, 2 and 3, probably due to the high crystallinity of as-synthesized TiO_2 NPs (Fig. 4). Decrease in UV absorption due to depletion in the crystallinity, was reported before by Kim et al. [23]. However, Fig. 4 illustrates XRD patterns of samples 1, 2, 3 and pure TiO_2. According to the height of the TiO_2 peaks in Fig. 4, existence of PEG and/or Dex during HTP led to the formation of less crystallized particles in comparison with samples after HTP without any dispersant. As reported elsewhere [24], in dispersants-free samples, the rate of hydrolytic reaction is relatively high. However, in dispersant containing samples, a lot of un-hydrolyzed alkyls and dispersants were remained between TiO_2 oligomers. These remaining materials impede the amorphous to anatase phase transformation by adsorbing on the surfaces of TiO_2 NPs, therefore the degree of crystallinity decreases. On the other hand, Yu et al. found that the ether oxygen in PEG interacts with metal ions and affects the crystallization of TiO_2 [25].

The dispersion state and the long-term stability of the samples, as shown in Fig. 3, illustrate the suspensions 1, 4, 5 and 6 displaying the sedimentation against time. This means that these suspensions did not remain stable for at least 24 h. On the contrary, in samples 2 and 3, the decline in absorption over 60 days was near zero, which demonstrates that the samples have been stable and have undergone a poor sedimentation. The results show that Dex and PEG/Dex seem to be the efficient dispersants for deflocculation of TiO_2 NPs if added to starting materials before the HTP.

3.2. Determination of crystalline phases

According to Fig. 4, although the main peak of the anatase phase [JCPDS: 86-1156] ($2\theta = 25.335^\circ$) is near to one of the main peaks of triethylamine hydrochloride [JCPDS: 9-548]

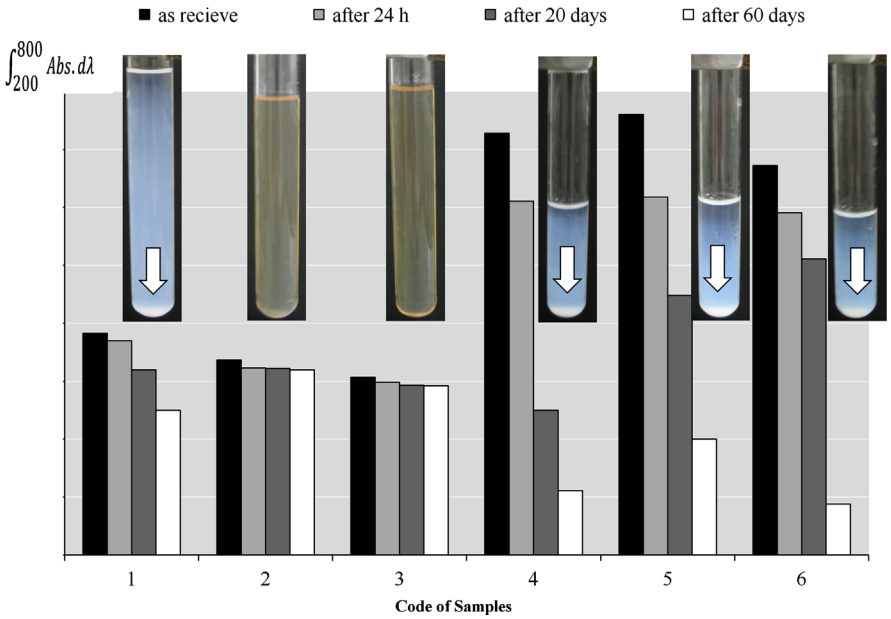

Fig. 3. Absorbance of nano TiO_2 suspensions as a function of relaxation time (0, 24 h, 20 and 60 days), accompanied with their visual dispersion state after 60 days.

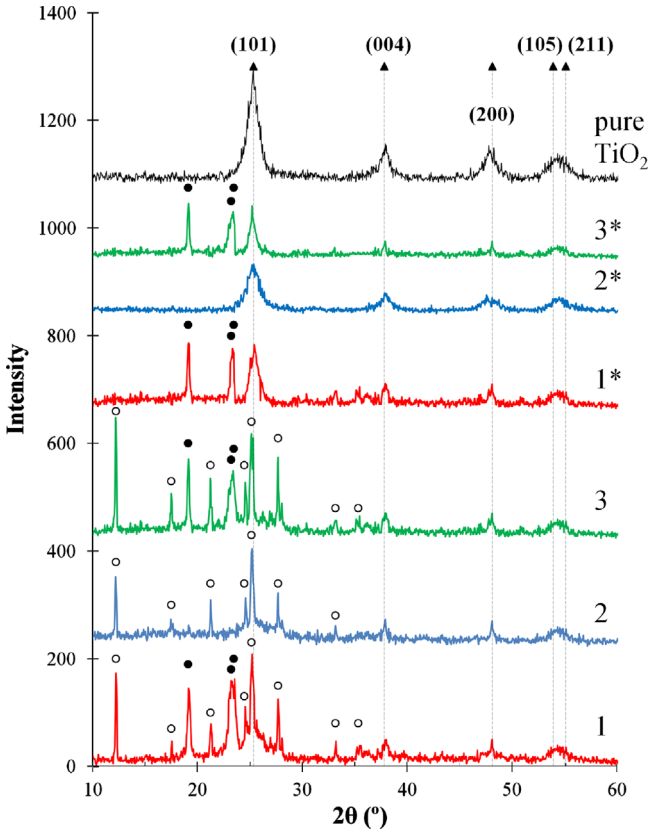

Fig. 4. XRD patterns of samples 1–3 before and after dialysis process. 1^*, 2^* and 3^* refer to samples 1, 2 and 3 after dialysis process, respectively. ●: PEG [JCPDS: 50-2158], ▲: anatase [JCPDS: 86-1156] and ○: triethylamine hydrochloride [JCPDS: 9-548].

($2\theta = 25.136°$), the formation of TiO_2 in samples 1, 2 and 3 is evident due to the existence of some short peaks at 37.809°, 48.104°, 53.921° and 55.138° (Fig. 4). Furthermore, XRD patterns of these three samples after using a dialysis membrane (MWCO = 5000, against distilled water) to make triethylamine hydrochloride penetrate out, demonstrating the formation of TiO_2 NPs owning less crystallinity (Fig. 4: 1^*, 2^* and 3^*). However, the crystallinity of the samples 1, 2 and 3 was less than that of samples 4, 5 and 6, as described before.

According to XRD results, the formation of TiO_2 in the samples is ascertained. In order to show the formation of bonding between NPs and dispersants and also the weight proportion of NPs to dispersant, FTIR and TGA were utilized.

3.3. FTIR

A careful analysis of FTIR spectra of pure TiO_2, PEG, Dex and samples 1–6 is shown in Fig. 5. Based on the literature [18], the characteristic absorption band of TiO_2 NPs at 400–600 cm^{-1} is attributed to Ti–O bond. The traces of this bond could be found in all 6 samples.

The band at 3502 cm^{-1} is due to the hydroxyl (OH) stretching vibration. The bands at 2884, 1642 and 1106 cm^{-1} correspond to C–H, C=O and C–O stretching vibrations, respectively. The characteristic absorption band at 961 cm^{-1} belongs to –CH out-of-plane bending vibrations of PEG [18,21,26]. Additionally, the absorption bands that occur at 1471, 1344, 1282 and 1242 cm^{-1} are due to CH, CH_2 and CH_3 bending vibrations, respectively [27]. By comparing the FTIR spectra of pure PEG and TiO_2 NPs with PEG in both methods (samples 1 and 4), the formation of intense bonding between PEG and NPs is improbable.

The representative absorption peaks of Dex including 3322 cm^{-1} (O–H stretching vibration), 2937 cm^{-1} (stretching vibration of CH_2 groups), 1674 cm^{-1} (C=O stretching vibration), 1447 cm^{-1} (C–H bending vibration), 1156, 1110 and 1014 cm^{-1} (stretching vibration of the alcoholic hydroxyl (C–OH))

are explicitly observed in the FTIR spectrum of pure Dex [14,28]. In comparison to pure Dex, some new peaks exist in the spectrum of sample 2. For example, the peak at 1773 cm^{-1} is ascribed to the C=O stretching vibration and the peak centered at 542 cm^{-1} is attributed to the Ti-O bond [14,18,28,]. In the spectrum of sample 5, with the exception of the band centered at 562 cm^{-1} that is related to Ti–O bond, no new peak is observed. All of these evidences prove that in the first method, Dex had been successfully conjugated to the surface of NPs via interaction between the functional group of Dex and the surface hydroxyl groups of TiO_2, whereas in the second method, a strong bonding between NPs and Dex had not been created.

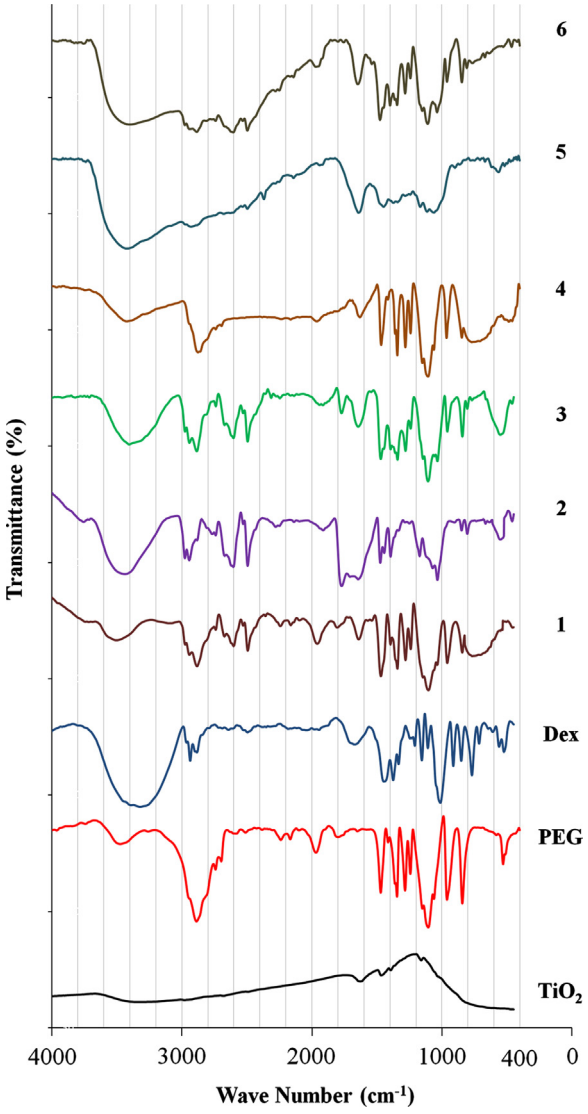

Fig. 5. FTIR spectra of pure TiO_2, PEG, Dex and samples 1–6.

In samples 3 and 6 (containing PEG, Dex and NPs), almost all the characteristic peaks of pure PEG and Dex and also the peak at 462 cm^{-1} that is ascribed to Ti–O bond, existed. As explained for sample 2, new bonding has appeared in sample 3 at 1773 cm^{-1} that is attributed to C=O stretching vibration [28]. These proofs corroborate that the interaction between NPs and dispersant agents in the first method is more vigorous than that in the second method.

The results of FTIR investigations are in good agreement with the consequences of stability assessments (Fig. 3). Long-term stable samples (Fig. 3, samples 2 and 3) were those samples illustrating a new bonding between NPs and dispersant in FTIR results.

3.4. TGA

Fig. 6 shows the TGA curves of the samples (passed across dialysis membrane, MWCO = 5000, against distilled water) under atmospheric conditions. The weight losses of the modified NPs and also pure PEG and Dex are shown in this figure. The weight loss was not observed in pure TiO_2 because of drying before TGA (not shown). For all the samples, a great weight loss started above 300 °C due to the decomposition and oxidation of polymeric materials. According to the inset of Fig. 6, the residual mass of pure PEG and Dex is about zero; therefore, since the dispersants were decomposed completely, the residual material is mostly TiO_2 NPs. The percentage of dispersant was gained in the TGA curves as ~75 wt% in sample 1, ~51 wt% in sample 2 and 58 wt% in sample 3.

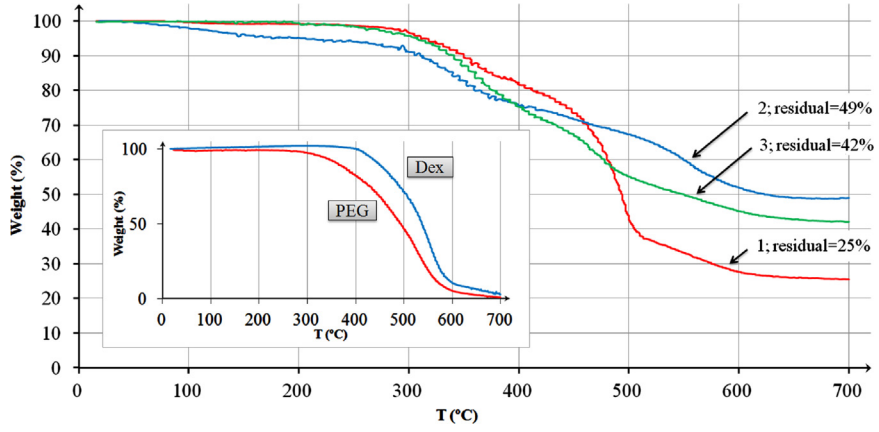

Fig. 6. TGA curves of samples 1, 2 and 3. The inset shows TGA curves of pure PEG and Dex.

According to Table 1, weight percent of dispersants in all samples must be 50. TGA results showed that in sample 1, the percentage of PEG increases to 75. It must be noted that during dialysis process, NPs pass the membrane unless they are conjugated to huge polymeric molecules. Decrease in residual mass in sample 1% to 25% reveals that ~66% of TiO_2 NPs has been removed from the membrane due to the lack of appropriate linkage between NPs and PEG. This phenomenon led to the sedimentation of NPs as it is shown in Fig. 3.

In sample 2, residual percentage up to 49% is close to the expected value (50%) refers to binding interaction between the functional group of Dex and the surface hydroxyl groups of TiO_2; therefore, the amount of NPs passing across the membrane is close to zero. Formation of bonding between Dex and NPs is evident with regards to Figs. 3 and 5 too.

In sample 3, despite decreasing the amount of Dex to 25 wt% (see Table 1), residual percentage (42%) is close to the expected value (50%), which indicates that the small amount of Dex (in comparison to sample 2) could reduce removing NPs (to ~27% of TiO_2 NPs) during dialysis process.

3.5. Morphology observations and SAED investigations

With the purpose of perusing microstructures and morphology of pure and also modified NPs, TEM and HRTEM were utilized. Micrographs of samples are shown in Fig. 7. Fig. 7(a) illustrates TEM image of pure TiO_2 and reveals distinct irregularly spherical particles and rod-like crystals with a size distribution ranging from 5 to 20 nm. NPs seem to be aggregated forming compact clusters in absent of dispersants to stabilize them. The agglomeration facilitates sedimentation (Fig. 3). Fig. 7(b) shows TEM image of sample 1. The existence of PEG during HTP caused the formation of semi spherical grains with the particle size about 10 nm. XRD results confirm that the characteristic peaks of pure TiO_2 have been weakened and broadened in sample 1 (Fig. 4). Decrease in particle size due to addition of PEG was also reported by Tan et al. [29]. PEG molecules are known to adsorb onto TiO_2 oligomers by forming hydrogen bonds in the sol–gel process, preventing preferred growth on crystallization [30], and also facilitating the inorganic polymerization degree [29]. Comparison between part (a) and (b) in Fig. 7 demonstrates that although NPs aggregation slightly declines in PEG containing specimen (sample 1), but existence of chain-like clusters is obvious, indicating that PEG could not cover NPs and prevent agglomeration perfectly. This fact could be deduced via FTIR results in Fig. 5, too.

HRTEM images in Fig. 7(c) and (d) confirm that the surface of NPs (samples 2 and 3) has been coated by dispersant to form a core-shell structure. No significant agglomeration was seen in these samples due to the effective coating of NPs (Fig. 5).

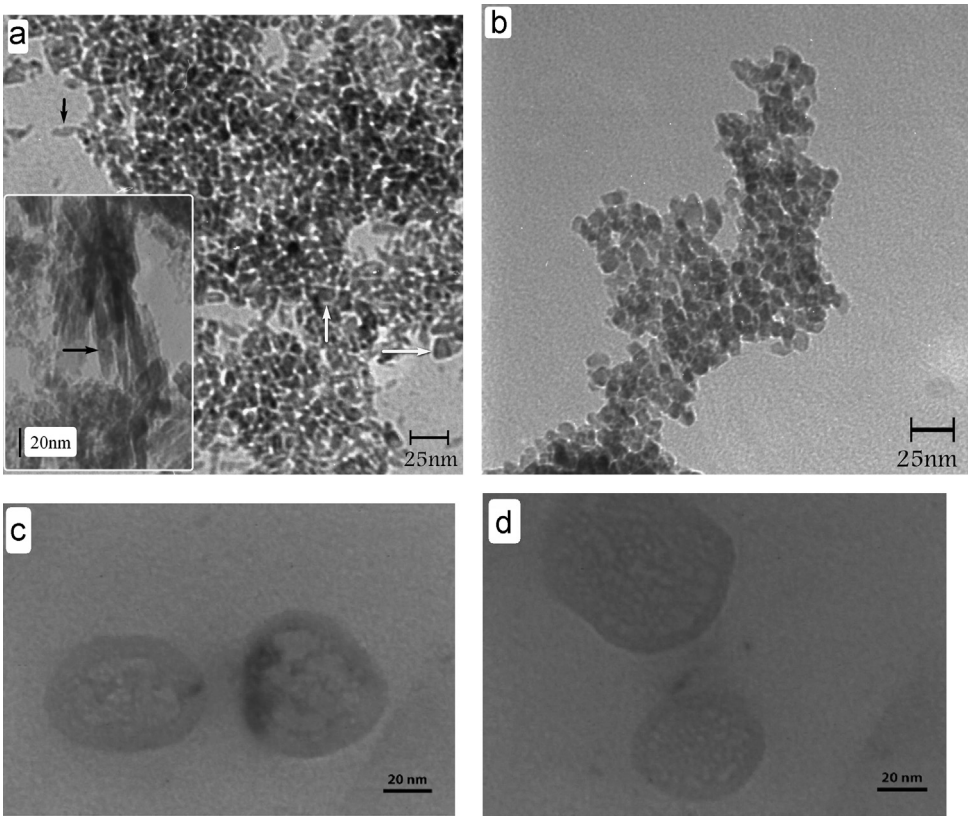

Fig. 7. Microscopic images of pure TiO_2 and samples 1, 2 and 3. (a) TEM image of pure TiO_2, the inset shows HRTEM image of this sample. (b) TEM image of sample 1. (c) HRTEM image of sample 2. (d) HRTEM image of sample 3.

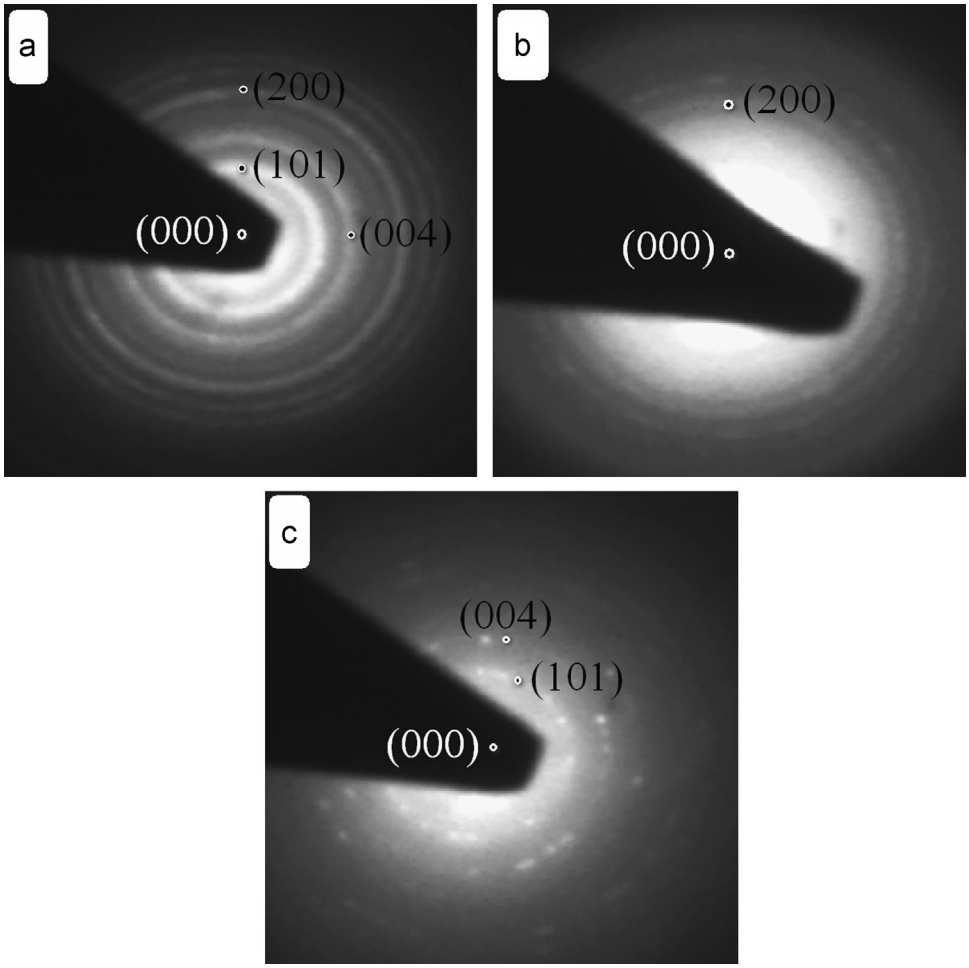

Fig. 8. ED patterns of (a) pure TiO_2, (b) sample 2 and (c) sample 3.

The suspended NPs could not contact with each other due to spatial repulsion of polymeric dispersant; therefore, tendency of sedimentation decreases remarkably (Fig. 3). It must be noted that in samples 2 and 3, the NPs are in semi spherical shape providing high amount of surface area. On the other hand, the thicknesses of polymeric layer on NPs are about 10 and 7 nm in samples 2 and 3, respectively.

Fig. 8 illustrates electron diffraction (ED) patterns of pure TiO_2 and samples 2 and 3. The crystallinity of the pure TiO_2 was more than that of the others as seen in the XRD patterns (Fig. 4). In comparison to pure TiO_2, the ED patterns of samples 2 and 3 showed obscured and spotty rings, respectively. Pure TiO_2 reveals sharp and clear rings indicating good crystalline perfection (Fig. 8a). Sample 2 demonstrates obscured rings (Fig. 8b) due to the low degree of crystallinity. In the case of sample 3, the existence of spotty rings (Fig. 8c) refers to the further decrease in crystallinity (see Fig. 4).

According to Fig. 8(a), the *d*-values corresponding to the most intense rings were in agreement with the standard *d*-values for the (101), (004) and (200) planes of the anatase phase [JCPDS: 86-1156]. In Fig. 8(b), one can find just an intense ring referring to (200). In Fig. 8(c), these rings are spotty; suggesting that the crystalline domains that make up this sample had not been arranged well as explained in the discussion of XRD results.

4. Conclusion

Two methods were used for modification of TiO_2 NPs in order to improve their colloidal stability in a water base medium. Addition of dispersants to as-synthesized NPs by hydrothermal assisted sol–gel method (second method) delayed the sedimentation up to 24 h, whereas Dex and Dex/PEG coated NPs during HTP (first method) did not show any tendency of sedimentation at least for 60 days.

In the first method, PEG could not improve the suspension stability of NPs due to lack of appropriate bonding between NPs and PEG. TGA results demonstrated that more than half of NPs could not conjugated to PEG and passed through the dialysis membrane. The penetrating out of NPs during dialysis remarkably decreased due to the formation of adequate bonding in the modified NPs by Dex and PEG/Dex.

Although both of the introduced methods led to the formation of anatase phase, the degree of crystallinity of the first method was less than that of the second one.

Agglomeration in PEG which modified NPs via the first method was evident in TEM images. Covering the NPs by Dex and PEG/Dex (core-shell structure) in samples prepared by the first method was obvious in HRTEM images. The thicknesses of polymeric shells in these samples were estimated to be ~10 and ~7 nm, respectively.

The formation of anatase phase and reduction of the degree of crystallinity in the samples prepared by the first method were corroborated by SAED results.

References

[1] W. Han, Y. Wang, Y. Zheng, In vivo biocompatibility studies of nano TiO_2 materials, Advanced Materials Research 79–82 (2009) 389–392.

[2] W. Han, Y. Wang, Y. Zheng, In vitro biocompatibility study of nano TiO_2 materials, Advanced Materials Research 47–50 (2008) 1438–1441.

[3] O. Carp, C.L. Huisman, A. Reller, Photoinduced reactivity of titanium dioxide, Progress in Solid State Chemistry 32 (2004) 33–177.

[4] K. Hashimoto, H. Irie, A. Fujishima, TiO_2 photocatalysis: a historical overview and future prospects, Japanese Journal of Applied Physics 44 (2005) 8269–8285.

[5] Y. Qin, L. Sun, X. Li, Q. Cao, H. Wang, X. Tang, L. Ye, Highly water-dispersible TiO_2 nanoparticles for doxorubicin delivery: effect of loading mode on therapeutic efficacy, Journal of Materials Chemistry 21 (2011) 18003–18010.

[6] M. Signoretto, E. Ghedini, V. Nichele, F. Pinna, V. Crocella, G. Cerrato, Effect of textural properties on the drug delivery behaviour of nanoporous TiO_2 matrices, Microporous and Mesoporous Materials 139 (2011) 189–196.

[7] S. Yamaguchi, H. Kobayashi, T. Narita, K. Kanehira, S. Sonezaki, N. Kudo, Y. Kubota, S. Terasaka, K. Houkin, Sonodynamic therapy using water-dispersed TiO_2 polyethylene glycol compound on glioma cells: comparison of cytotoxic mechanism with photodynamic therapy, Ultrasonics Sonochemistry 18 (2011) 1197–1204.

[8] J.H. Lee, M. Kang, S.J. Choung, K. Ogino, S. Miyata, M.S. Kim, J. Y. Park, J.B. Kim, The preparation of TiO_2 nanometer photocatalyst film by a hydrothermal method and its sterilization performance for *Giardia lamblia*, Water Research 38 (2004) 713–719.

[9] T.Y. Lai, W.C. Lee, Killing of cancer cell line by photoexcitation of folic acid-modified titanium dioxide nanoparticles, Journal of Photochemistry and Photobiology A 204 (2009) 148–153.

[10] M. Song, R. Zhang, Y. Dai, F. Gao, H. Chi, G. Lv, B. Chen, X. Wang, The in vitro inhibition of multidrug resistance by combined nanoparticulate titanium dioxide and UV irradiation, Biomaterials 27 (2006) 4230–4238.

[11] Q. Li, X. Wang, X. Lu, H. Tian, H. Jiang, G. Lv, D. Guo, C. Wu, B. Chend, The incorporation of daunorubicin in cancer cells through the use of titanium dioxide whiskers, Biomaterials 30 (2009) 4708–4715.

[12] R. Yang, H. Yu, M. Li, Mesoporous properties of nanosized anatase titania powders prepared by urea hydrolysis with PEG dispersant, Journal of Materials Science Letters 22 (2003) 1131–1135.

[13] S. Naghibi, A. Jamshidi, O. Torabi, R. Ebrahimi K., Application of Taguchi method for characterization of corrosion behaviour of TiO_2 coating prepared by sol–gel dipping technique, International Journal of Applied Ceramic Technology, http://dx.doi.org/10.1111/ijac.12077, in press.

[14] M. Shi, J. Shen, H. Ma, Z. Li, X. Lu, N. Li, M. Ye, Preparation of grapheme-TiO_2 composite by hydrothermal method from peroxotitanium acid and its photocatalytic properties, Colloids and Surfaces A 405 (2012) 30–37.

[15] Z.E. Allouni, M.R. Cimpan, P.J. Hol, T. Skodvin, N.R. Gjerdet, Agglomeration and sedimentation of TiO_2 nanoparticles in cell culture medium, Colloids and Surfaces B 68 (2009) 83–87.

[16] M.C. Garnett, P. Kallinteri, Nanomedicines and nanotoxicology: some physiological principles, Occupational medicine 56 (2006) 307–311.

[17] S.S. Mano, K. Kanehira, S. Sonezaki, A. Taniguchi, Effect of polyethylene glycol modification of TiO_2 nanoparticles on cytotoxicity and gene expressions in human cell lines, International Journal of Molecular Sciences 13 (2012) 3703–3717.

[18] S. Luo, F. Wang, Z. Shi, F. Xin, Preparation of highly active photocatalyst anatase TiO_2 by mixed template method, Journal of Sol–Gel Science and Technology 52 (2009) 1–7.

[19] R.S. Petryshyn, Z.M. Yaremko, M.N. Soltys, Effects of surfactants and pH of medium on zeta potential and aggregation stability of titanium dioxide suspensions, Colloid Journal 72 (2010) 517–522.

[20] N. Veronovski, P. Andreozzi, C. La Mesa, M. Sfiligoj-Smole, V. Ribitsch, Use of Gemini surfactants to stabilize TiO_2–P_{25} colloidal dispersions, Colloid and Polymer Science 288 (2010) 387–394.

[21] Y. Zhang, N. Kohler, M. Zhang, Surface modification of superparamagnetic magnetite nanoparticles and their intracellular uptake, Biomaterials 23 (2002) 1553–1561.

[22] C.J. Brinker, G.W. Scherer, Sol–Gel Science; The Physics and Chemistry of Sol–Gel Processing, Academic Press, Waltham, Massachusetts, USA, 1990.

[23] D.S. Kim, S.Y. Kwak, The hydrothermal synthesis of mesoporous TiO_2 with high crystallinity, thermal stability, large surface area, and enhanced photocatalytic activity, Applied Catalysis A 323 (2007) 110–118.

[24] G. Wang, Hydrothermal synthesis and photocatalytic activity of nanocrystalline TiO_2 powders in ethanol–water mixed solutions, Journal of Molecular Catalysis A: Chemical 274 (2007) 185.

[25] K. Yu, J. Zhao, Y. Guo, X. Ding, H. Bala, Y. Liu, Z. Wang, Sol–gel synthesis and hydrothermal processing of anatase nanocrystals from titanium *n*-butoxide, Materials Letters 59 (2005) 2515–2518.

[26] J. Zhang, S. Rana, R.S. Srivastava, R.D.K. Misra, On the chemical synthesis and drug delivery response of folate receptor-activated, polyethylene glycol-functionalized magnetite nanoparticles, Acta Biomater 4 (2008) 40–48.

[27] K. Kavkler, N. Gunde-Cimerman, P. Zalar, A. Demsar, FTIR spectroscopy of biodegraded historical textiles, Polymer Degradation and Stability 96 (2011) 574–580.

[28] H. Bai, Z. Liu, D.D. Sun, Highly water soluble and recovered dextran coated Fe_3O_4 magnetic nanoparticles for brackish water desalination, Separation and Purification Technology 81 (2011) 392–399.

[29] R. Tan, Y. He, Y. Zhu, B. Xu, L. Cao, Hydrothermal preparation of mesoporous TiO_2 powder from $Ti(SO_4)_2$ with poly(ethylene glycol) as template, Journal of Materials Science 38 (2003) 3973–3978.

[30] K. Kajihara, K. Nakanishi, K. Tanaka, K. Hirao, N. Soga, Preparation of macroporous titania films by a Sol–Gel dip-coating method from the system containing poly (ethylene glycol), Journal of the American Ceramic Society 81 (1998) 2670–2676.